THE DYNAMICAL EVOLUTION OF THE DUST SHELL OF IRC +10 216

R. OSTERBART[1], Y. BALEGA[2], T. BLÖCKER[1], A. MEN'SHCHIKOV[3], G. WEIGELT[1]

[1] *Max–Planck–Institut für Radioastronomie, Bonn, Germany*
[2] *Special Astrophysical Observatory, Nizhnij Arkhyz, Russia*
[3] *Stockholm Observatory, Saltsjöbaden, Sweden*

ABSTRACT. We present high–resolution J–, H–, and K–band observations of the carbon star IRC +10 216. The images were reconstructed from 6 m telescope speckle interferograms using the bispectrum speckle interferometry method. The H and K images consist of several compact components within a 0.2" radius and a fainter asymmetric nebula. The brightest four components are denoted with A to D in the order of decreasing brightness. A comparison of our images gives — almost like a movie of five frames — insight to the dynamical evolution of the inner nebula. For instance, the separation of the two brightest components A and B increased by almost 40% from 191 mas in 1995 to 265 mas in 1998. At the same time, component B is fading and the components C and D become brighter. The X–shaped bipolar structure of the nebula implies an asymmetric mass–loss suggesting that IRC +10 216 is very advanced in its AGB evolution, shortly before turning into a protoplanetary nebula. The cometary shape of component A suggests that the core of A is not the central star, but the southern lobe of a bipolar structure. The position of the central star is probably at or near the position of component B.

1. Introduction

IRC +10 216 (CW Leo) is the nearest and best–studied carbon star and one of the brightest infrared sources. It experiences strong mass-loss rates of $\dot{M} \approx 2 - 5 \times 10^{-5} M_\odot \, \mathrm{yr}^{-1}$ (Loup et al. 1993). The central star of IRC +10 216 is a long–period variable with a period of ~ 649 days (Le Bertre 1992). Recent distance estimates range from 110 pc to 150 pc (Groenewegen 1997, Crosas & Menten 1997). IRC +10 216's initial mass can be expected to be close to $4 \, M_\odot$ (Guelin et al. 1995, Weigelt et al. 1998). The bipolar appearance of the nebula around this object was already reported, e.g., by Kastner & Weintraub (1994). The non-spherical structure is consistent with the conjecture that IRC +10 216 is in a phase immediately before entering the protoplanetary nebula stage. The most recent high–resolution observations of this object and its circumstellar dust shell were reported by Weigelt et al. (1998), Haniff & Buscher (1998), and Tuthill et al. (1999). The results of Dyck et al. (1991) and Haniff & Buscher (1998) showed that the dust-shell structure of IRC +10 216 is changing within some years.

2. Observations and bispectrum speckle interferometry results

The IRC +10 216 speckle interferograms were obtained with the 6 m telescope at the Special Astrophysical Observatory in Russia. At all continuum epochs data within

the K–band were obtained (date / center wavelength of the filter in μm / FWHM bandwidth of the filter in μm: 8.10.95/2.12/0.02, 3.4.96/2.17/0.02, 23.1.97/2.19/0.41, 14.6.98/2.17/0.33, 3.11.98/2.19/0.19). J- and H-band data were recorded at one epoch (2.4.96/1.24/0.28, 23.1.97/1.64/0.31) each.

Figures 1 and 2 show the K, H, and J images of the central region of IRC +10 216 for all epochs. The high–resolution images were reconstructed from the speckle interferograms using the bispectrum speckle interferometry method (Weigelt 1977, Lohmann et al. 1983, Weigelt 1991). We denote the resolved components in the center of the nebula as A, B, C, and D (see Fig. 2b) in the order of decreasing peak intensity (based on the K band results from 1996). Figure 2b shows in addition three fainter components denoted with E, F, and G. The faint extended feature at position angle PA $\sim$340° in the J image corresponds quite well to the faint component E visible in all images in Figs. 1 and 2 (assuming that the brightest component in the J image is coinciding with component A in the H and K images, see Figure 3a).

Figure 3 shows the results of polarimetric observations with the HST Nicmos camera at a wavelength of 1.1 μm (raw data retrieved from the Hubble Data Archive, STScI). The data were obtained at a photometric phase of $\Phi = 0.76$. From the data the total intensity (Figs. 3a and b), the polarized intensity (Fig. 3c), the degree and position angle of the polarization (Fig. 3b) have been derived.

3. Nebula structures

The bright inner region of IRC +10 216 is surrounded by a larger faint nebula. The bipolar shape of this nebula is most prominently present in the J–band image (Fig. 2c) and in the HST images at shorter wavelengths (Fig. 3a). However, the fact that even in the polarized intensity the nebula is very faint on the southeastern side suggests the main axis of the nebula to be at PA$\sim$ 20° to 30° along the direction from component A to B. This fits well to the main axis of the $H^{13}CN(J = 1 - 0)$ emission (Dayal & Bieging 1995) which is weakly elongated on a scale of about 10″.

We determined the separations of the components A and B for the 5 epochs from 1995 to 1998 shown in Fig. 1. The separations are: 191 mas, 201 mas, 214 mas, 245 mas, and 265 mas. A linear regression fit gives a value of 23 mas/yr for the average increase in the apparent separation of the components. Interpreting this increase as a real motion would lead to 14 km/s within the plane of the sky (for a distance of 130 pc). The result comprises data from more than one pulsation period ($\sim$649 days, see Le Bertre 1992) and it is thus obvious that the apparent relative motion of the nebula components is not simply related to the stellar variability.

Besides the motion of the components, Fig. 1 shows that these components change their shapes and relative fluxes. The brightest component A becomes narrower along the axis A–B ($\sim$20°). The peak–to–peak intensity ratio of B and A is almost constant from 1995 to 1997. Later component B is fading. At the same time the other components become brighter and detached from A. Note that the photometric phases and the integral K magnitudes of IRC +10 216 in January 1997 and November 1998 are almost identical (Osterbart et al. 1999). Again we find that the time scale for the changes seen in our images is significantly different from the period of the stellar pulsation.
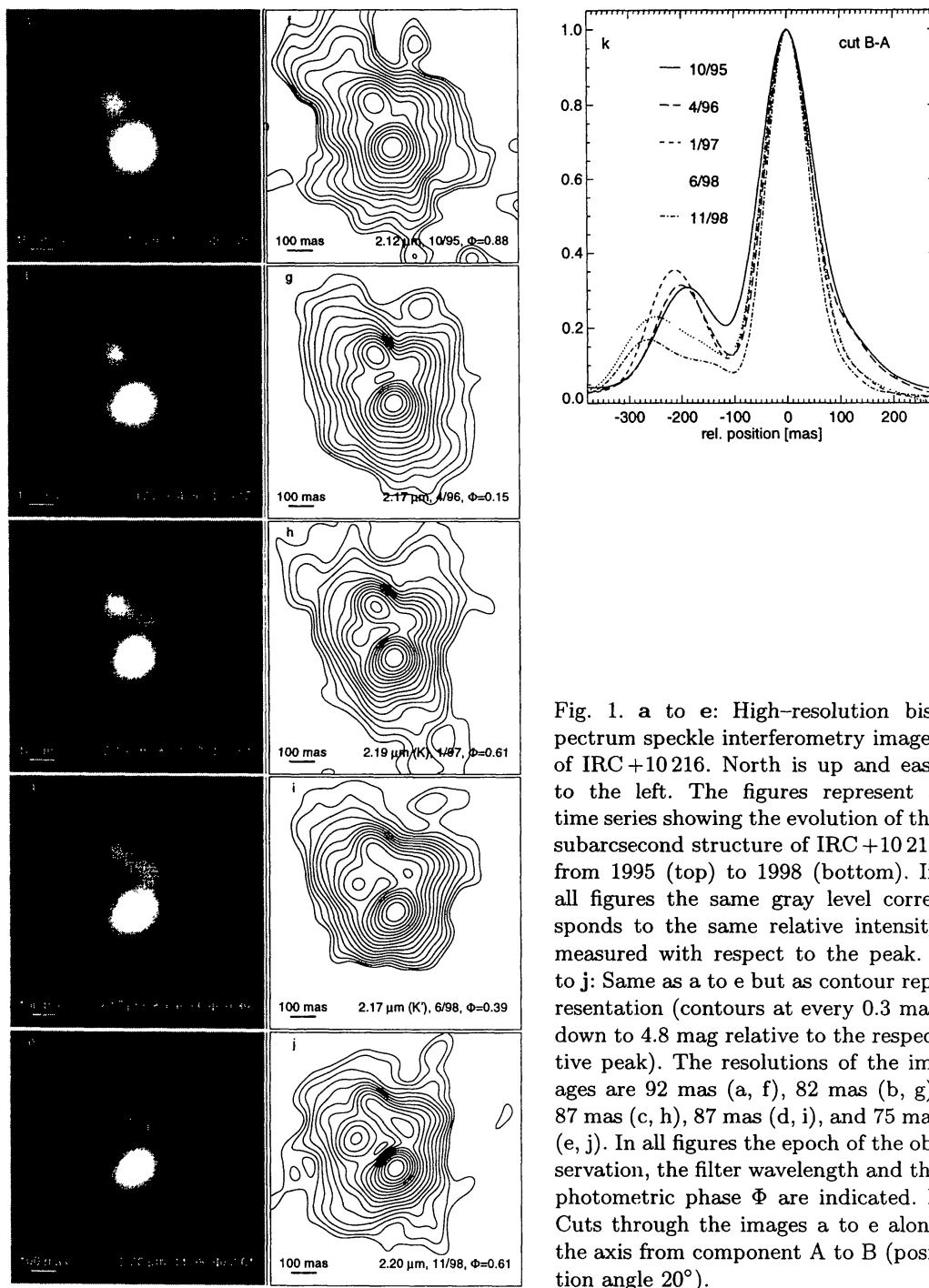
100 mas   2.12 µm, 10/95, Φ=0.88

100 mas   2.17 µm, 4/96, Φ=0.15

100 mas   2.19 µm (K), 1/97, Φ=0.61

100 mas   2.17 µm (K'), 6/98, Φ=0.39

100 mas   2.20 µm, 11/98, Φ=0.61

k   cut B-A

— 10/95
-- 4/96
--- 1/97
6/98
-·- 11/98

1.0

0.8

0.6

0.4

0.2

0.0

-300   -200   -100   0   100   200

rel. position [mas]

Fig. 1. **a** to **e**: High–resolution bispectrum speckle interferometry images of IRC +10 216. North is up and east to the left. The figures represent a time series showing the evolution of the subarcsecond structure of IRC +10 216 from 1995 (top) to 1998 (bottom). In all figures the same gray level corresponds to the same relative intensity measured with respect to the peak. **f** to **j**: Same as a to e but as contour representation (contours at every 0.3 mag down to 4.8 mag relative to the respective peak). The resolutions of the images are 92 mas (a, f), 82 mas (b, g), 87 mas (c, h), 87 mas (d, i), and 75 mas (e, j). In all figures the epoch of the observation, the filter wavelength and the photometric phase Φ are indicated. **k** Cuts through the images a to e along the axis from component A to B (position angle 20°).
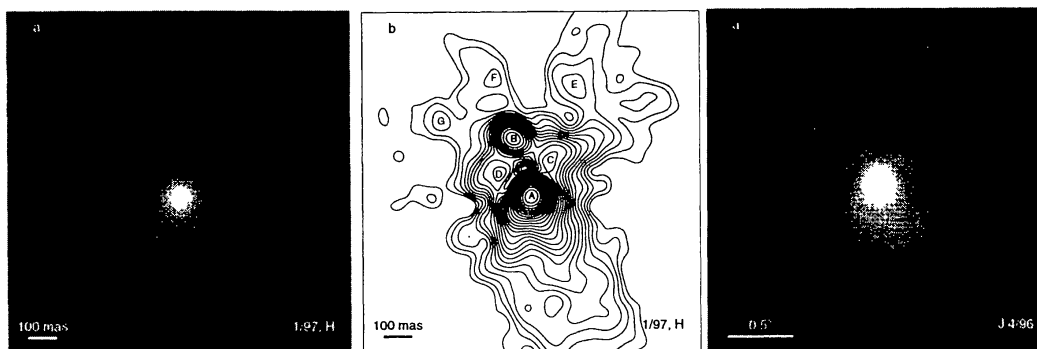
Fig. 2. **a** 70 mas resolution bispectrum speckle interferometry image of IRC +10 216 in the *H*–band. North is up and east to the left. **b** Same as (a) as a contour image with denotations (A to G) of compact structures. Contours are at every 0.2 mag down to 5.0 mag relative to the peak. **c** *J*–band speckle reconstruction of IRC +10 216 with 149 mas resolution.
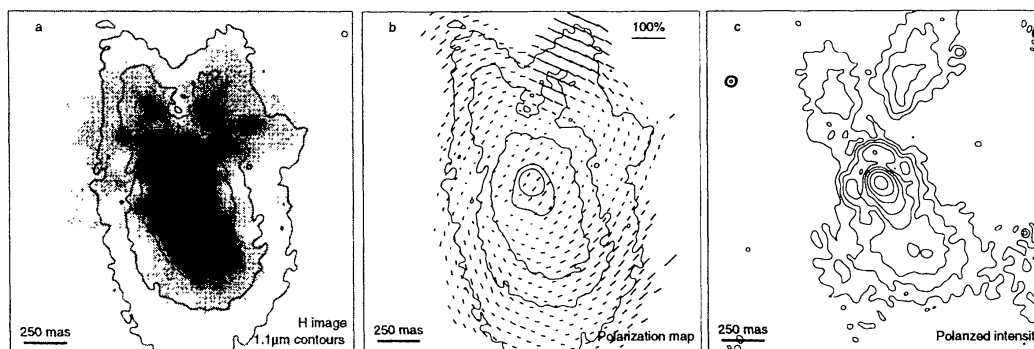

Fig. 3. **a** Superposition of the total intensity at 1.1 μm (contours are at 5.0, 4.2, 3.4, 1.8, and 1.0 mag relative to the peak) derived from the archival HST polarization data and the negative *H* speckle image. **b** 1.1 μm polarization map. The same contours as in frame a are shown. **c** Polarized intensity at 1.1 μm. The contours are plotted from 2.4 mag to 6.0 mag difference relative to the peak of the total intensity in steps of 0.6 mag. The structure of the polarization data at the position of B is affected by the diffraction pattern associated with A.

4. Discussion

In the following we want to address the question where, behind all the dust, the central star in the system of IRC +10 216 is located. This question is of specific interest to understand the physical properties of the nebula. At short wavelengths the nebula shows a bipolar structure. A comparison of the observed structure to other bipolar nebulae like the Red Rectangle (Men'shchikov et al. 1998) suggests that the X–like arms originate mainly from scattering of stellar light on the surfaces of cavities. The star then is at least partially obscured by an optically thick dust shell or torus. Convincingly Haniff & Buscher (1998) argued that the main axis of the object is tilted with its southern side

towards the observer.

Is component A the star? At first glance it seems reasonable to assume that the star is at the position of the brightest component A. However, the synthetic polarization maps of Fischer et al. (1996) show that a significant polarization at the position of the star is only present for nearly edge–on configurations. The high degree of polarization of A ($P \sim 14\%$) is thus not in agreement with A being the star because the structure of the bipolar nebula at short wavelengths suggests that we are looking at an intermediate viewing angle (e.g. 50° to 60°). At larger separations from A the polarization pattern is centrosymmetric. The center of such a pattern is thought to be at the position of the illuminating source (Fischer et al. 1996). Since in the map in Fig. 3b this center does not coincide with A, but is located significantly north of A, we are led to the conclusion that A is not the star.

Is the star at the position of B? In the following we will show that it is consistent with the observation to assume that the star is at the position of B.

(a) The cometary shapes of A (Fig. 2) as well as the presented polarization data strongly suggest that A is part of a scattering lobe within a bipolar structure. Consistently, component A and its southern tails are relatively blue ($H - K$ in the range from 2 to 3.2; see Osterbart et al. 1999) compared to the integral color ($H - K = 3.2$).

(b) The northern components B, C, and D are, on the other hand, rather red ($H - K \approx 4.2$) in comparison with the integral color. This suggests that these structures are strongly obscured and reddened by circumstellar dust.

(c) The brightest northern component in the J image (Fig. 2c) can hardly be seen in the H image and is thus very blue. This component and A can be considered as opposite lobes of an almost bipolar structure. Component B is almost in the center between these counterlobes and thus approx. at the position where the star would be expected.

(d) The polarization map (Fig. 3b) fits well to the picture that the star is at B. The center of the centrosymmetric polarization pattern at larger separations from A is located between the two J–band lobes. This is consistent with the assumption that the illuminating source is at or near the postion of B (cf. Fischer et al. 1996). Unfortunately, the polarization at the position of B itself is contaminated by contributions from the diffraction pattern associated with the peak A.

Changes in the mass loss rate. The change of the shape of component A and the fading of B can be attributed to an increasing mass loss which is accompanied by a gradual increase of the optical depth of the dust shell. This is most obvious for the later observation epochs, suggesting an enhanced mass loss since 1997. A strongly variable mass loss has, in fact, been predicted by theoretical models treating the dust formation mechanism in the envelopes of long–period variable carbon stars (Winters et al. 1995). Periods of this mechanism may be significantly longer than the stellar pulsation period.

Alternative models: the star between A and B or near B. It is not possible to exclude that the star may be located between A and B, close to B, or in the center of A, B, C, and D. The precision of the polarization map is not sufficient to conclude whether the star is at the position of B or only close to it. Two–dimensional radiative transfer calculations in progess show, however, that the observed intensity ratio of A and B as well as the components' shapes clearly require the star to be at B.

5. Stellar evolution and bipolar structure

IRC +10 216 is without doubt in a very advanced stage of its AGB evolution due to its long pulsational period, high mass-loss rate, and carbon-rich dust-shell chemistry indicating that already a significant number of thermal pulses did take place. The star's initial mass can be estimated to be $4M_\odot \pm 1M_\odot$ due to the observed isotopic ratios of C, N and O in the dust shell (Guelin et al. 1995) and the luminosity of the central star (Weigelt et al. 1998). Accordingly, the core mass should be ~ 0.7 to $0.8M_\odot$ with corresponding thermal-pulse cycle times of $\sim 1 - 3\,10^4$yr (Blöcker 1995). Introducing the mean observed mass-loss rate to these thermal-pulse periods shows that the present stellar wind leads to a very effective erosion of the envelope per thermal pulse cycle, possibly as high as $\sim 1M_\odot$/cycle. Consequently, the whole envelope may be lost during the next few thermal pulses leading to the termination of the AGB evolution. Thus, it is not unlikely to assume that IRC +10 216 has entered a phase immediately before moving off the AGB. This is strongly supported by the non-spherical appearence of its dust shell showing even bipolar structures. Unlike AGB stars, post-AGB objects as protoplanetary nebulae often expose prominent features of asphericities, in particular in axisymmetric geometry (e.g. Olofsson 1996). Accordingly, IRC +10 216 can be thought to be an object in transition. It is noteworthy that the establishment of bipolar structures, i.e. the metamorphosis into a protoplanetary nebula, obviously already begins during the (very end of) AGB evolution. The clumpiness within the bipolar shape is probably due to small scale fluctuations of the dust condensation radius which, in turn, might be influenced by, e.g., giant surface convection cells (Schwarzschild 1975). The formation of giant convection cells can be assumed to be a common phenomenon in red giants.

The shaping of planetary nebulae can successfully be described by interacting stellar wind models (Kwok et al. 1978). Within this scenario a fast (spherical) wind from the central star interacts with the slow wind of the preceding AGB evolution. The slow AGB wind is asssumed to be non-spherical (axisymmetric) which leads to the observed morphology of planetary nebulae (Mellema 1996). Different mechanisms to provide the required equatorial density enhancements are discussed (cf. Livio 1993). Among these, binarity is one channel including common envelope evolution and spin up of the AGB star due to the interaction with its companion (Morris 1981). Not only stellar companions are found to be able to spin up the AGB star but also substellar ones as brown dwarfs and planets, most effectively by evaporation in the AGB star's envelope (Soker 1997). Currently there is no observational evidence for a possible binary nature of IRC +10 216. The fact that the polarization pattern in the southeastern part of the nebula at 1.1 μm has a different orientation than in the rest of the nebula might be an indication for a second illuminating source.

Mechanisms inherent to the star include rotation, non-radial pulsations, and magnetic fields (see e.g. Dorfi & Höfner 1996, Soker & Harpaz 1992, Garcia-Segura et al. 1999). Both non-radial p-modes and magnetic fields appear to be only important for significant rotation rates. Often spin-up agents due to binarity are assumed. For instance, Groenewegen (1996) favours non-radial pulsation or a yet unidentified companion which spun up the central star as the most likely explanation for the non-spherical shape of the dust shell of IRC +10 216.

AGB stars are known to be slow rotators. Stars with initial masses below $\sim 1.3 M_\odot$ can be expected to lose almost their entire angular momentum during the main sequence phase due to magnetic braking operating in their convective envelopes. Consequently they are not believed to develop non-spherical mass-loss due to rotation. Stars with larger initial masses are spun down due to mass loss but may achieve sufficiently high rotation rates at the end of AGB evolution (Garcia-Segura et al. 1999). Already small rotation rates influence dust-driven winds considerably yielding a mass loss preferentially driven in the equatorial plane (Dorfi & Höfner 1996). For supergiants leaving the Hayashi line Heger & Langer (1998) found that significant spin up of the surface layers may take place. Thus, at second glance, rotation might be able to support axisymmetric mass loss during the transition to the proto-planetary nebula phase for AGB stars as IRC +10 216.

6. Conclusions

We have presented high-resolution $J-$, $H-$, and $K-$band observations of IRC +10 216 with the highest resolution so far at H of 70 mas. A series of $K-$band images from five epochs between October 1995 and November 1998 shows that the inner nebula is non-stationary. The separations of the four dominant resolved components increased within the 3 years by almost $\sim 40\%$. For the two brightest components a relative velocity within the plane of the sky of about 23 mas/yr or 14 km/s was found. Within these 3 years the rather faint components C and D become brighter whereas component B is fading. The general geometry of the nebula seems to be bipolar.

We find that the most promising model to explain the structures and changes in the inner nebula is to assume that the star is at the position of component B. The star then is strongly but not totally obscured at H and K. Consistently component B is very red in the $H - K$ color while A and the northern $J-$band components are relatively blue. Similarly the polarization pattern with strong polarization in the northern arms and still a significant polarization in the peak supports this model. The inner nebula and the apparent motions seem to be rather symmetric around this position and the observed changes are consistent with an enhanced mass loss since 1997.

IRC +10 216 is without doubt in a very advanced stage of its AGB evolution. The observed bipolarity of its dust shell even reveals that it has possibly entered the phase of transformation into a protoplanetary nebula.

References

Blöcker, T.: 1995, *Astron. Astrophys.* **297**, 727
Crosas, M., Menten, K. M.: 1997, *Astrophys. J.* **483**, 913
Dayal, A., Bieging, J. H.: 1995, *Astrophys. J.* **439**, 996
Dorfi, E., Höfner, S.: 1996, *Astron. Astrophys.* **313**, 605
Dyck, H. M., Benson, J. A., Howell, R. R., Joyce, R. R., Leinert, C.: 1991, *Astron. J.* **102**, 200
Fischer, O., Henning, T., Yorke, H. W.: 1996, *Astron. Astrophys.* **308**, 863
Garcia-Segura, G., Langer, N., Rozyczka, M., Franco, J.: 1999, *Astrophys. J.* **517**, 767
Groenewegen, M. A. T.: 1996, *Astron. Astrophys.* **305**, L61

Groenewegen, M. A. T.: 1997, *Astron. Astrophys.* **317**, 503

Guelin, M., Forestini, M., Valiron, P., Ziurys, L. M., Anderson, M. A., Cernicharo, J., Kahane, C.: 1995, *Astron. Astrophys.* **297**, 183

Haniff, C. A., Buscher, D. F.: 1998, *Astron. Astrophys. Lett.* **334**, L5

Heger, A., Langer, N.: 1998, *Astron. Astrophys.* **334**, 210

Kastner, J. H., Weintraub, D. A.: 1994, *Astrophys. J.* **434**, 719

Kwok, S., Purton, C.R., Fitzgerald, P.M.: 1978, *Astrophys. J. Lett.* **219**, L125

Le Bertre, T.: 1992, *Astron. Astrophys. Suppl. Ser.* **94**, 377

Livio, M.: 1993, in *Planetary Nebulae*, R. Weinberger, A. Acker (eds.), Dordrecht: Kluwer, p. 279

Lohmann, A. W., Weigelt, G., Wirnitzer, B.: 1983, *Appl. Opt.* **22**, 4028

Loup, C., Forveille, T., Omont, A., Paul, J. F.: 1993, *Astron. Astrophys. Suppl. Ser.* **99**, 291

Mellema, G.: 1996, *Astrophys. Space Sci.* **245**, 239

Men'shchikov, A., Balega, Y., Osterbart, R., Weigelt, G.: 1998, *New Astron.* **3**, 601

Morris, M.: 1981, *Astrophys. J.* **249**, 572

Olofsson, H.: 1996, *Astrophys. Space Sci.* **245**, 169

Osterbart, R., Balega, Y. Y., Blöcker, T., Men'shchikov, A. B., Weigelt, G.: 1999, *Astron. Astrophys.* , submitted

Schwarzschild, M.: 1975, *Astrophys. J.* **195**, 137

Soker, N., Harpaz, A.: 1992, *Publ. Astr. Soc. Pacific* **104**, 923

Soker, N.: 1997, *Astrophys. J. Suppl.* **112**, 487

Tuthill, P. G., Monnier, J. D., Danchi, W. C.: 1999, in *AGB stars*, Le Bertre T., Lèbre A., Waelkens C. eds., *IAU symp.* 191, *ASP Conf. Ser.*, Provo: ASP, p. 331

Weigelt, G.: 1977, *Optics Commun.* **21**, 55

Weigelt, G.: 1991, in *Progress in Optics*, Wolf, E. ed., Vol. 29, North Holland, p. 293

Weigelt, G., Balega, Y. Y., Blöcker, T., Fleischer, A. J., Osterbart, R., Winters, J. M.: 1998, *Astron. Astrophys.* **333**, L51

Winters, J. M., Fleischer, A. J., Gauger, A., Sedlmayr, E.: 1995, *Astron. Astrophys.* **302**, 483